

# Low-Voltage Ge Avalanche Photodetector for Highly Sensitive 10Gb/s Si Photonics Receivers

H. T. Chen<sup>1,2</sup>, P. Verheyen<sup>1</sup>, M. Rakowski<sup>1,3</sup>, P. De Heyn<sup>1,2</sup>, G. Lepage<sup>1</sup>, J. De Coster<sup>1</sup>, P. Absil<sup>1</sup>, G. Roelkens<sup>2</sup>,

J. Van Campenhout<sup>1</sup>

<sup>1</sup>IMEC, Kapeldreef 75, Leuven, Belgium,

<sup>2</sup>Photonics Research Group, Department of Information Technology, Ghent University - imec, Ghent B-9000, Belgium

<sup>3</sup>ESAT-MICAS, K.U. Leuven Kasteelpark Arenberg 10 B-3001 Leuven, Belgium

**Abstract**— We demonstrate low-voltage germanium waveguide avalanche photodetectors (APD) with gain-bandwidth product of 88GHz. A 7.1dB sensitivity improvement is demonstrated for an APD wire-bonded to a 10Gb/s CMOS transimpedance amplifier, at -6.2V APD bias.

**Index Terms**— Avalanche photodetector; Optical interconnects; Silicon photonics

## I. INTRODUCTION

Avalanche photodetectors (APDs) integrated in a Si photonics platform offer great potential to improve the performance of Si-based optical interconnects. By leveraging the internal gain of the APD, optical receivers can be realized with significantly improved optical sensitivity as compared to conventional PIN photodetector based receivers. Key performance metrics for APDs include multiplication gain and excess noise. High avalanche gain with low excess noise has been demonstrated in surface Ge detectors in a Separate Absorption, Charge, and Multiplication (SACM) configuration using Ge as light absorption layer and Si as multiplication layer [1], enabling impressive gain-bandwidth product of 340GHz and -28dBm receiver sensitivities at 10Gb/s. However, such implementation requires a high bias voltage of around -25V, which is not compatible with CMOS supply voltages.

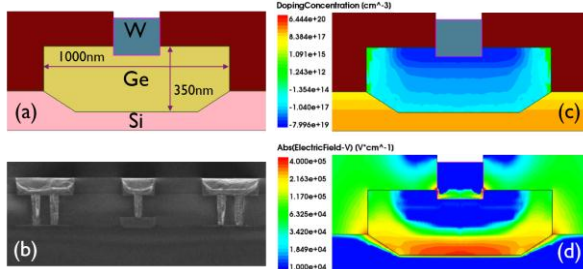


Figure 1. (a) Schematic cross-section of the Ge waveguide APD. (b) SEM cross section image. (c) Simulated doping distribution. (d) Simulated electric field distribution at -3.0V applied voltage.

Recently, strong avalanche gain was reported at low voltages (-3V) [2] in waveguide APDs comprised of a thin Ge layer with metal-semiconductor-metal (MSM) contacts. Strongly non-uniform electric fields generated by the interdigitated contacts vias were exploited to mitigate the intrinsically poor avalanche excess-noise properties of bulk Ge. However, the large dark current of the MSM device and poor primary responsivity strongly limited the receiver sensitivity.

In this paper, we demonstrate a PIN based Ge waveguide APD and explore opportunities to simultaneously enable high gain, low noise, low dark current and low operation voltage, by engineering a thin Ge multiplication layer [2,3] in a vertical PIN structure.

## II. DEVICE STRUCTURE AND FABRICATION PROCESS

The Ge waveguide APDs are implemented in imec's fully integrated Si Photonics Platform along with Si modulators [4] and various passive devices, utilizing a sub-set of 130nm CMOS processing modules in addition to selective Ge epitaxial growth and Ge chemical-mechanical planarization, on 200mm SOI wafers with 220nm top silicon and 2μm buried oxide. The cross-sectional dimensions of the Ge APD are shown in Fig. 1(a). A vertical PIN (VPIN) diode is formed by implanting Si with phosphorous ions (before Ge growth) and the planarized Ge layer with boron ions, resulting in a dopant profile as shown in Fig. 1(c). This heterogeneous Ge/Si VPIN diode configuration results in a strongly non-uniform electric field as high as  $3 \times 10^5$  V·cm<sup>-1</sup> at -3.0V, tightly confined in the lower ~100nm of the Ge layer as shown in Fig. 1(d). Hence, it is expected that strong avalanche multiplication can take place at moderate applied bias, and that part of the avalanche excess-noise generation can be suppressed [2,3].

## III. DEVICE CHARACTERISTICS

A typical static current-voltage characteristic of a

$10.4\mu\text{m}$ -long VPIN Ge APD device is shown in Fig. 2(a). The device has a low dark current of  $28.7\text{nA}$  at  $-2.0\text{V}$ . The breakdown voltage, defined at a dark current of  $10\mu\text{A}$ , occurs at  $-6.4\text{V}$ . Light current is measured at  $1550\text{nm}$  wavelength with an input optical power of  $-18.9\text{dBm}$  received by the germanium photodiode. The responsivity is constant from  $0\text{V}$  to  $-3.5\text{V}$ , owing to the relatively large built-in electrical field that sweeps out the majority of the photo-generated carriers. The measured primary responsivity is  $0.53\text{A/W}$ . Next, the reverse bias voltage is increased, resulting in significantly higher light and dark current. The light-current gain is extracted by normalizing to the light current at  $-2.0\text{V}$ , and is shown in Fig. 2(b). It can be seen that at  $90\%$ ,  $95\%$  and  $98\%$  of the breakdown voltage, the light-current gain is  $3.4$ ,  $6.5$  and  $14.8$  respectively.

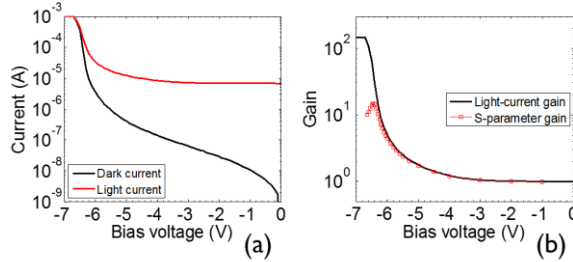


Figure 2. (a) I-V characteristics of a  $10.4\mu\text{m}$  length Ge APD. (b) Static light-current avalanche gain and small-signal avalanche gain.

Next, small-signal radio-frequency (RF) measurement are carried out on the APD. The  $S_{21}$  parameter at  $1550\text{nm}$  wavelength with input optical power of  $-19.2\text{dBm}$  is shown in Fig. 3(a) for various applied bias voltages. It can be seen that the low-frequency gain increases with bias voltage until  $-6.45\text{V}$ . Beyond this voltage, avalanche gain is reduced. Also, it can be seen that the 3-dB bandwidth reduces substantially with increasing bias voltage. Both avalanche gain and 3-dB bandwidth extracted from the  $S_{21}$  curves are shown in Fig. 3(b). At low bias, the bandwidth is as high as  $50\text{GHz}$  (setup limitation) and remains constant as long as the gain is smaller than 2. As gain increases, the bandwidth drops inversely proportional owing to the avalanche build-up time [5]. At  $-6.2\text{V}$  APD bias, a gain of  $7.2$  and a gain-bandwidth product of  $88\text{GHz}$  is obtained.

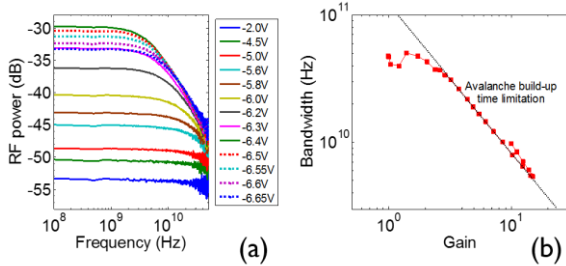


Figure 3. (a) Small-signal RF measurement of  $S_{21}$  parameter at different bias voltages. (b) 3-dB bandwidth vs. gain from  $S_{21}$  curves.

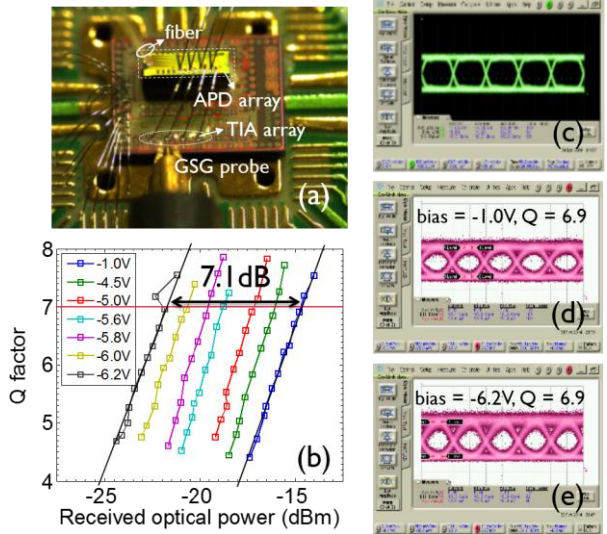


Figure 4. (a) Ge waveguide APD array, wire-bonded to a CMOS TIA array. (b) Measured electrical Q factor vs. received optical power and APD bias voltages. (c)  $10\text{Gb/s}$  reference optical eye diagram. (d)  $10\text{Gb/s}$  eye diagram at  $-1.0\text{V}$ . (e)  $10\text{Gb/s}$  eye diagram at  $-6.2\text{V}$ .

#### IV. APD RECEIVER CHARACTERISTICS

Next, the APD is wire-bonded to a  $10\text{Gb/s}$  transimpedance amplifier (TIA), as shown in Fig. 4(a). The TIA is implemented in  $40\text{nm}$  LP CMOS [6]. The APD receiver sensitivity was estimated by launching an optical pseudo-random bit sequence (PRBS) data pattern at  $10\text{Gb/s}$  ( $2^{31}-1$  word length), generated by a commercial modulator with  $12.5\text{dB}$  extinction ratio, into the APD. The TIA electrical output is subsequently displayed on a high-speed oscilloscope, and the Q factor of the electrical eye diagram is recorded for various average optical power levels and various APD bias, as shown in Fig. 4(b). At  $-1\text{V}$  APD bias, the waveguide-referred sensitivity is estimated to be  $-14.9\text{dBm}$  average optical power ( $Q\sim 7$ ), mostly limited by the TIA input-referred noise current estimated to be  $\sim 2.4\text{ }\mu\text{A}$ . At  $-6.2\text{V}$  APD bias voltage, a  $7.1\text{dB}$  sensitivity improvement is obtained (absolute receiver sensitivity of  $-22.0\text{dBm}$ ). Wide open eye diagrams at APD biases of  $-1.0\text{V}$  and  $-6.2\text{V}$  are shown in Fig. 4(d) and 4(e), further illustrating the ability of the APD to generate  $>7\text{dB}$  gain with low excess noise.

In summary, we demonstrated a Ge waveguide APD with  $88\text{GHz}$  gain-bandwidth product, enabling  $7\text{dB}$  receiver sensitivity improvement at  $10\text{Gb/s}$  at low APD bias of  $-6.2\text{V}$ . This work was supported by imec's CORE partner program.

- [1] Kang, Y. et al., *Nature Photon.* 3, 59–63 (2009).
- [2] Assefa, S. et al., *Nature* 464, 80–84 (2010).
- [3] Hayat, M. M. et al., *Trans. Electron Devices* 49, 2114–2123 (2002).
- [4] Pantouvaki, M. et al., *ECOC Conf.* (2013), We.3.B.2.
- [5] Emmons, R. B. et al., *J. Appl. Phys.* 38, 3705–3714 (1967).
- [6] Rakowski, M. et al., *IEEE Optical Interconnect Conf.* (2014).